Forest Ecology and Management 587 (2025) 122750

Contents lists available at ScienceDirect

Forest Ecology and Management

journal homepage: www.elsevier.com/locate/foreco

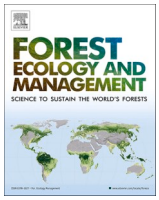

Post-fire vegetation regeneration during abnormally dry years following severe montane fire: Southern Alberta, Canada

J. Aspinall, L. Chasmer *, C.A. Coburn, C. Hopkinson

Department of Geography and Environment, University of Lethbridge, Lethbridge, AB T1K 3M4, Canada

ARTICLE INFO

Keywords:
Fire regime
Biomass
Remotely piloted aircraft systems (RPAS)
Structure from motion
Drought
Wildfire
Mountain

ABSTRACT

Fire regimes across montane regions of western Canada are changing resulting in longer fire seasons, higher intensity fires, and shortening fire return intervals. The implications of high severity fire and warmer, drier early post-fire conditions on herbaceous understory vegetation regeneration and seedling recruitment in the southern Canadian Rockies are not well known. The overall objective of this study is to quantify trajectories of vegetation recovery (species, structural characteristics, and biomass) during early years of abnormally warm, dry conditions following a high severity fire in two moisture endmember sites Waterton Lakes National Park, Alberta, Canada. Here, we compare the within and between year spatial and temporal variability of vegetation growth and species density and how these change over time and across the broader area as an indicator of ecosystem resilience within these endmember sites. Moderate to extreme drought occurred during the years following fire at Waterton, where 2021 was ranked as the 2nd driest year in 26 years. Despite this, the moist site was characterised by greater herbaceous vegetation recovery with few lodgepole pine seedlings (average biomass = 335 g m^{-2}), while a drier site had greater seedling recruitment over a period of 5 years. Variations in site environmental conditions were more impactful than differences between years (drought) on post-fire vegetation recovery. Use of remotely piloted aircraft system (RPAS) remotely sensed data provided an effective means for quantifying variability in regenerating vegetation height (structure from motion), cover (green chromatic coordinate), and biomass when compared at plot level (R^2 = 0.53, 0.53, and 0.30 respectively) using optical photogrammetric methods. The research presented has implications for forest and fuel management in Canada as national parks and forest agencies consider historic use of heterogeneous species patches. High density of lodgepole pine seedling recruitment in mineral soils and under very dry conditions indicate resilience to drought. This will require continued and expanded monitoring as other tree species recruits populate the post-fire environment.

1. Introduction

The spatial and temporal dynamics of fire disturbance in mountain forest ecosystems across western Canada and the United States are changing as a result of climatic, management history, and compounding disturbances such as mountain pine beetle (e.g. Daniels et al., 2011; Haughian et al., 2012). These changes are resulting in greater and relatively unknown post-fire effects on vegetation recruitment and recovery in mountain sites in western Canada. Post-fire vegetation recruitment and seedling density in the first few years are largely influenced by life history (Tackle, 1959) and the availability of serotinous cones especially from *Pinus contorta* (Lodgepole pine), an early successional species (Turner et al., 1997; Talucci et al., 2019). Fire characteristics are also important, where lodgepole pine seedling density generally increases with fire severity (Lotan et al., 1985; Assal et al., 2021), and also depending on fire behaviour and intensity. In mountain pine beetle impacted stands in British Columbia burned by fire, for example, Talucci et al. (2019) found that seedling recruit density was higher than that in fire refugia but was lower in crown fire impacted stands and greater in stands with ground fire. Post-fire seedling recruitments also depend on topoedaphic and hydrological drivers of post-fire recovery. Schoennagel et al. (2003) found greater numbers of recruits in low elevation areas of Yellowstone National Park with low fire return intervals (>100 years). Lodgepole pine also inhabit soils that may not be appropriate for other species in the early years following fire as these areas can go through periods of saturation/ponding (Lotan

* Corresponding author.
E-mail address: laura.chasmer@uleth.ca (L. Chasmer).

https://doi.org/10.1016/j.foreco.2025.122750
Received 14 October 2024; Received in revised form 15 April 2025; Accepted 18 April 2025
Available online 25 April 2025

et al., 1985). High rates of recovery of lodgepole pine have also been observed on dry mineral soils (Tackle, 1959) which vary with disturbance and various biotic and abiotic drivers (Talucci et al., 2019).

. While the post-fire recovery of mountain forests in western North American have been studied since the early 20th century (e.g. Fisher, 1935) less is known about the impacts of increasingly warmer and drier climate and micro-site conditions on early site recovery. The early years are important: 70–90 % of regeneration may occur within the first 10 years (Stevens-Rumann et al., 2022). Above-average snowpack accumulation and cool, wet summers in the years following fire may enhance vegetation recruitment and survival (Andrus et al., 2018). Lotan et al. (1985) describe positive influence of snowmelt on germination of seedlings; Talucci et al. (2019) found a negative relationship between both snow and dry conditions and seedling recruitment. Soil moisture is dependent on soil bulk density, macropore development, and post-fire vegetation growth. Feddema et al. (2013) observed higher mortality of *Pseudotsuga menziesii* (Douglas fir) associated with drier soil conditions. Littlefield (2019) found that lodgepole pine growth increased in the year following a warm July and Harvey et al. (2016) found seedling recruitments of various mountain species declined with greater severity of drought. Over a longer period of post-fire chronosequences, Guz et al. (2021) found that drought had little influence on lodgepole pine recruitment as seedlings can survive with little moisture and reduced snowpack. While moisture variability can be important, seed source had the greatest impact on seedling density in their study.

Early successional herbaceous understory plants also respond rapidly to fire via surviving belowground propagules associated with the burned area patch size (Turner et al., 1997). These can contribute to biodiversity, nutrient cycling, energy balance, and soil development of the post-fire environment and are influenced by the physical and chemical properties of soil, where higher diversity is found in areas with high site index (Chen et al., 2004). In Chen et al. (2004) high light availability and low limits on nutrients and moisture were not significant enough to result in competitive exclusion and homogeneity in understory species. Post-fire environmental drivers operate in the context of pre-fire ecosystem attributes, and fire severity can influence the composition and biodiversity of regenerating vegetation communities (Coop et al., 2010). Further, water runoff and evaporative losses can lead to displacement/desiccation of seeds reducing survival (Rother, 2015), especially during prolonged dry periods. The complexity of these interacting drivers is acute in mountain ecosystems where steep terrain and abrupt hydro-climatic gradients result in distinct ecotones over comparatively short distances (Feddema et al., 2013).

This study quantifies intra-seasonal, phenological, and inter-annual trajectories of understory herbaceous vegetation and conifer establishment and growth during the first five years following high severity fire in Waterton Lakes National Park, Alberta, Canada. We also examine the sensitivity of early successional species and pine seedling recruitment to drought within endmember moist and dry sites using field data collected at rapid intervals. To quantify biomass change over larger areas, we test the efficacy of RPAS for vegetation productivity monitoring by comparing plot data with vegetation height/growth and cover over time as an easily acquired additional source of information on post-fire vegetation structural heterogeneity. Here, drought provides a proxy for the ecological impacts of fire as the climate continues to warm and dry and as droughts become more prevalent.

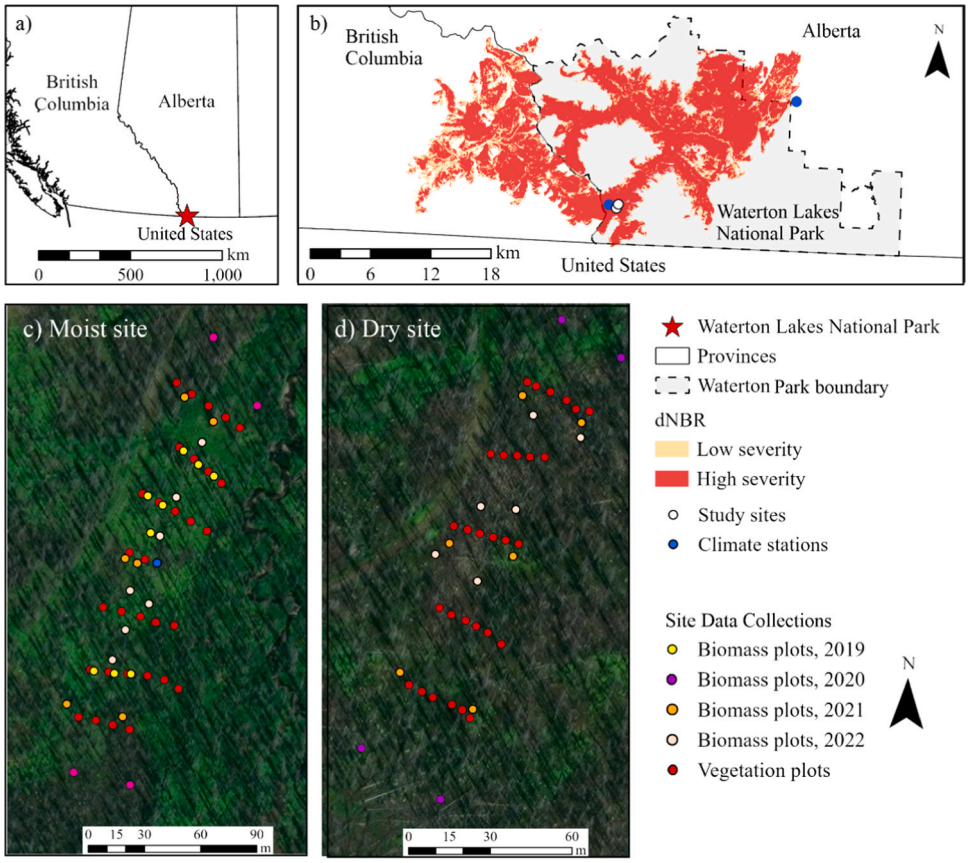

Fig. 1. a) Location of Waterton Lakes National Park within western Canada; b) location of two study sites and severity of the Kenow Wildland Fire from Landsat OLI-derived differenced Normalised Burn Ratio (dNBR) within British Columbia and Alberta as it extended through the park; c) and d) illustrate the location of biomass and vegetation plots within the moist and dry sites (overlaid onto Earthstar Geographics (Maxar) imagery).

2. Material and methods

2.1. Study area

This study was conducted within the southern Canadian Rocky Mountains in the Cameron Valley, Waterton Lakes National Park (hereafter 'Waterton') (114° 2' 24" W, 49° 1' 58" N), Alberta, Canada (Fig. 1a). The climatology of Waterton is characterized as humid continental with a mean annual air temperature of 2.4 °C and high annual precipitation for the mountain region of southern Alberta and British Columbia (~1072 mm) (Environment Canada, 2022).

Prior to the fire, trees within the Cameron Valley were older than 100 years, with no recorded natural or prescribed burns in the area during that time (Parks Canada, 2021). Barrett (1996) (in Axelson et al., 2018) suggest that the fire return interval in lower elevation valleys was 98 years with mixed severity fires occurring within 33–56 years (30 % of forests). Pre-fire tree species included mostly lodgepole pine, *Abies lasiocarpa* (subalpine fir), and Engelmann spruce (Parks Canada, 2018). The extirpation of the Indigenous population during the late 1800's/early 1900's and subsequent fire suppression over the last century led to the homogenization and maturity of forest species, typical to that of many recreational areas along the eastern slopes of the Canadian Rocky Mountains (Hessburg et al., 2019). This resulted in significant accumulation of biomass and soil organic matter prior to the fire (Gerrand et al., 2021). The Kenow Wildland Fire started from a lightning strike west of the Park in British Columbia on August 30, 2017, and spread over the continental divide into Waterton Lakes National Park on September 11, 2017, burning approximately 38 % (19,303 ha) of the Park's land area (Parks Canada, 2019). The high intensity of the fire was associated with a prolonged period of abnormally dry conditions and high wind speeds following ignition.

Two adjacent montane previously forested (burned) sites were selected to represent distinct topographical and moisture conditions within the Cameron Valley bottom, ~ 500 m north of Cameron Lake (Fig. 1c and d). 60 permanent vegetation microplots (area = 1 m^2) were installed at both sites, where 31 plots in the moist site were established in 2019, and 29 plots in the dry site were established in 2020 (Fig. 2). These plots were used to understand changing vegetation phenology, to quantify rates and variations in seedling establishment, and for validation of RPAS data.

The moist site is characterized by rills, which result in the formation of intermittent streams fed by groundwater during the summer months and overland flow in spring (until approximately late June, Fig. 2b). The soils at both sites were dry relative to expected pre-fire conditions, with the moist site showing an average volumetric water content (VWC) range between 21 % and 25 % (SD ± 7.5–15.6 %) during wet periods and 9–14 % (SD ± 6–8 %) during dry periods of the post-fire growing season. The surface topography of the moist site is generally east-facing with a low slope (average = 4°). The soil has a silty texture with some exposed mineral soils in the southernmost transect of vegetation plots. Pre-fire mature tree species within the site included Englemann spruce (74 %), lodgepole pine (21 %), and subalpine fir (6 %) (Gerrand et al., 2021). Post-fire herbaceous species varied with time since fire, with dominant species including *Rubus parviflorus* (thimbleberry), *Poa pratensis* (Kentucky bluegrass), *Spiraea betulifolia* (white spirea), and *Alnus viridis* (green alder).

The dry site is approximately 350 m south of the moist site and is elevated by ~15 m relative to the moist site (Fig. 2c). The site is sloped (average = 5°) and unlike the moist site, has few rills and depressions. The soil composition includes rocky mineral soils with shallow organic material following fire, and overall, lower VWC than the moist site. The average VWC ranged from 9 and 12 % (SD ± 4.3–4.7 %) during moist periods and from 4.1 % to 5.2 % (SD ± 2.9–3.1 %) during dry periods. Based on terrain, soil bulk density and soil moisture, the sites are significantly different (F statistic = 29.8; $p < 0.001$). Pre-fire mature tree species density vary, where lodgepole pine, *Picea glauca* (white pine), and subalpine fir make up 60 %, 24 %, and 17 %, respectively, of trees within the moist site (Gerrand et al., 2021). Within the dry site, herbaceous vegetation cover was sparse in the years following the fire, with *Chamaenerion angustifolium* (fireweed) dominance in the first few years and the regeneration of lodgepole pine seedlings by year three. The average depth of burn at the two sites was 18.2 cm (moist) and 13.3 cm (dry), indicating considerable loss of organic matter and carbon from the fire, especially in the moist site where there was significant moss accumulation (Gerrand et al., 2021).

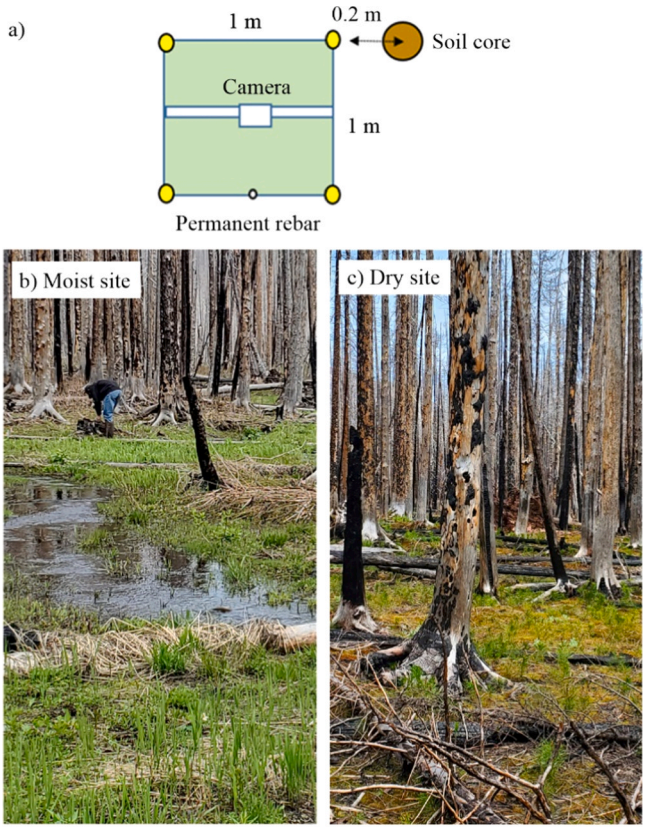

Fig. 2. a) Schematic diagram of a microplot setup within each site (illustrated in Fig. 1c and d as 'vegetation plots'). Microplots included a metal drop-down square frame, which was consistently positioned onto permanent rebar at the corners of each plot. The frame also included a constant height (1.8 m) metal bar to affix an RGB (red, green, blue) camera. A soil core was collected at each plot to determine spatial variations in soil bulk density; b and c) illustrate moist and dry site conditions in June 2022, including visible overland water characteristic of the moist site, whereas standing water was not observed at the dry site during any of the approximately bi-weekly measurements.

3. Data collection

3.1. Meteorological data

Air temperature and relative humidity were measured using a Campbell Scientific Inc. HMP45C (Fig. 1c) at 2 m above the ground surface. These were recorded at 15-minute intervals on a data logger installed at the moist site in October 2018 and averaged per 24-hr period. Precipitation data were measured using a Geonor all-season totalizing rain and snow gauge (Geonor, United States). Raw data were quality controlled to reduce sensor noise and corrected for wind-induced under-catch (Barnes and Hopkinson, 2022, data available in Hopkinson and Barnes, 2022). Complimentary air temperature, precipitation, and field-sampled snow water equivalent (SWE) data were also recorded at the nearby Alberta Environment and Protected Areas (AEPA) Akamina #2 climate station. This station is ~1.3 km west of and

~150 m higher in elevation than the study sites. The station was installed in 2018 following the Kenow fire (Agriculture and Irrigation, Alberta Climate Information Service (ACIS), 2021). Correspondence between gauge records at Akamina #2 and Cameron Valley is high (r^2 = 0.78). Annual total precipitation is ~1000 mm and most precipitation falls as snow during the winter months (Barnes et al., 2025).

Archived publicly available climate data measured at Waterton Park Gate (Environment Canada, 2022), 18 km north-east of the study sites were analysed to describe annual air temperature and precipitation deviations from the long-term mean as context for pre- and post-fire hydro-climatic conditions. Annual variations in air temperature were compared with the available 47-year mean, while water year (October to September) total precipitation data were compared with the available 26-year mean. A more localised assessment of pre- and post-fire climatic conditions was not possible due to the original AEPA station at Akamina (#1) being destroyed in the Kenow fire and the new Cameron and Akamina #2 sites being installed a year later within a very different non-vegetated post-fire landscape.

3.2. Early post-fire plot measurements

During the first post-fire season of 2018, multiple qualitative site visits allowed for establishment of sites for the field study, including plot locations and environmental sensing equipment. Vegetation monitoring plots were established in the north-east to south-west orientation of the Cameron Valley (prevailing wind direction) (Fig. 1c and d). Vegetation plots (Fig. 2a) were measured and photographed approximately bi-weekly. In 2019, vegetation measurements and RGB photography began during the last week in May (Julian Day (JD) 149) within the moist site, whereas in later years (2020–2022), measurements began during the 2nd week of June (about JD 160). Fewer measurements were completed in 2020 due to COVID-19 and site access constraints. All plots were located using a Topcon Inc. (Canada) HiPer SR II survey-grade Global Navigation Satellite System (GNSS), with either a kinematic 'stop and go' or 'rapid static' survey rover differentially corrected to a static reference base station located within 500 m of both sites.

Plot measurements included vegetation height measured at left, centre, and right sides of the plot using an extendable meter ruler, and canopy cover at the same (left, centre, right of plot locations) based on the point intercept method (Caratti, 2006). Vegetation genus and, where possible, species were identified including conifer seedling count/height starting in 2021. To determine soil bulk density within each plot, soil cores were collected in 2020 using an AMS soil core sampler kit (AMS, United States) and three liner inserts (each measuring 4.8 cm diameter and 5 cm depth). Soil cores were collected at three depth intervals (0–5 cm, 5–10 cm, and 10–15 cm). Each depth interval was separated by cutting the soil between the liner inserts and stored individually to identify changes in bulk density with depth. VWC (%) was also measured within each plot using a Hydrosense 2 Handheld Soil Moisture Sensor (Campbell Scientific Inc.).

Photographs of each plot were taken at time of measurement (within 4 hours of solar noon) using an RGB digital camera (Fig. 2a) to estimate canopy cover of regenerating vegetation and as a proxy indicator of productivity over time, based on the proportion of foliage to soil in each photograph. Downward-looking photographs were taken from approximately 1.8 m ± 0.2 m above each plot and covered the full area of the plot. To maintain consistent light conditions, during cloud-free or intermittent cloudy days, a large umbrella was used to simulate diffuse radiation conditions.

While height and cover are easily measured and compared between plots, biomass provides a more direct quantification of change related to differences in plant productivity. Here, biomass was harvested at both sites to develop biomass (and carbon) models and to calculate the rate of biomass accumulation over time with growth. Biomass across all classes of vegetation (herbaceous, shrub, seedlings) was harvested in surveyed plots throughout the sites at locations > 5 m from permanent micro-plots, so that micro-plots remained undisturbed. No location was harvested twice (Fig. 1c and d). A total of 26 and 16 microplots were harvested from the moist and dry sites, respectively. These were harvested from 2019 to 2022 for the moist site and from 2020 to 2022 for the dry site. All biomass plot locations were surveyed to within 0.10 m accuracy, so that biomass could be compared with RPAS optical imagery and structure from motion (SfM) photogrammetric data. All vegetation samples within the plots were clipped at the ground surface and stored in large paper bags for lab analysis.

3.3. RPAS data collection

Visible spectrum (RGB) photographs were collected bi-weekly to monthly, coincident with field measurements in fall 2018 and summers 2019, 2021, and 2022 using DJI Inc. Mavic Pro v1 (2018), Mavic Pro2 (2019, 2021), and the Matrice 300 (2022). RPAS data collections were excluded in summer 2020 due to COVID-19 restrictions. Data collections were used to determine the utility of RPAS data for spatially continuous modelling of vegetation growth and biomass accumulation. RPAS flight survey configurations are described in Table 1.

3.4. Airborne LiDAR data collection

Airborne LiDAR data were acquired annually in July or August within one week of RPAS data collections from 2018 through the study period (to 2022) using a Teledyne Optech Inc. Titan multi-spectral LiDAR with three laser return reflectance wavelengths: 532 nm, 1064 nm, and 1550 nm (e.g. Gerrand et al., 2021). LiDAR surveys were parameterized with a near constant flying height, scan angle, and pulse density to ensure comparability between years. In this study, LiDAR data were used minimally to create the DEM within eight months of the fire, to identify mature (burned) trees and tree canopies, and to align RPAS photogrammetric data.

4. Laboratory analysis of field samples

4.1. Vegetation plot and soil analysis

Vegetation height and cover were averaged per plot and per site (with standard deviation, SD). To assess spatial and temporal variations

Table 1
Specifications of RPAS data collections, including original pixel resolution, ground sample resolution, and point density of structure from motion (SfM) point clouds.

Date of collection	Site	RPAS and camera used (MP = megapixel)	Orthomosaic ground sample distance (cm)	Average point density (Points m^{-3})
Sept 6. 2018	Moist	Mavic Pro v1–4MP	1.16	1670
Aug 21, 2019	Moist	Mavic Pro2–20MP	0.89	3711
July 8, 2021	Moist	Mavic Pro2–20MP	1.40	986
Aug 29, 2021	Moist	Mavic Pro2–20MP	1.72	675
Aug 17, 2022	Moist	Zenmuse L1–20MP	1.90	3064
July 16. 2018	Dry	Mavic Pro v1–4 MP	1.16	1498
July 8, 2021	Dry	Mavic Pro2–20MP	1.22	1557
Aug 29, 2021	Dry	Mavic Pro2–20MP	1.57	995
Aug 18. 2022	Dry	Zenmuse L1–20MP	1.70	2935

in biomass and carbon accumulation between the two sites, harvested biomass was oven-dried at 60 °C until the weight of the biomass no longer fluctuated (approximately 48 hours). The carbon content of herbaceous vegetation was assumed to be 47.5 % of dry biomass weight (Zehetgruber et al., 2017).

Downwards-looking plot photographs were clipped to a consistent area and digital numbers (DNs) were extracted across RGB image bands. For each plot photograph, the photos were clipped to the size of the plot and DNs within each band were averaged and used to calculate the Green Chromatic Coordinate (herein PLOTgcc) (Woebbecke et al., 1995) for all plot photographs:

$$\text{PLOTgcc} = \frac{G}{(R + G + B)} \quad (1)$$

Where R, G, and B represent red, green, and blue bands, respectively within each photograph. To identify variation in phenology represented by vegetation height and PLOTgcc, the mean and standard deviation of all plot measurements in the moist and dry sites were included.

Soil cores were oven-dried at 105 °C for 24 hours or until the weight no longer changed (Carter and Gregorich, 2008). Dry soil weight and volume were used to calculate bulk density and compared with plot measurements.

5. Airborne remotely sensed data processing

5.1. RPAS image data processing

To remove image distortion and displacement, RPAS images collected in 2018 were processed to an orthomosaic in Pix4Dmapper, then further orthorectified, using ArcGIS Pro (ESRI, CA) to a 2018 airborne LiDAR-derived Digital Surface Model (DSM) collected over the length of the Cameron Valley. The remaining RPAS images (2019, 2021, 2022) were georeferenced to the 2018 RPAS image mosaic using 14–22 ground control points with 2nd-order polynomial transformation. The Root-Mean-Square Error (RMSE) for each image ranged from 0.07 m to 0.21 m and images were visually compared to ensure alignment of identifiable features. RGB bands were extracted per mosaic and used to calculate RPASgcc [Eq. 1]. Summary statistics: minimum, mean, maximum, and standard deviation were extracted from each vegetation plot and compared with PLOTgcc collected coincident to RPAS image collection. Similarly, RPASgcc was also extracted over the area of each biomass plot and compared with field measured biomass. Biomass was modelled from RPASgcc based on the 2nd order polynomial with a minimum of 0.33 RPASgcc as the origin (equal to 0), where RPASgcc < 0.33 was found in areas with no regenerating vegetation (e.g. in open water). The influence of overlying dead tree bole and canopy shadowing/3D height on vegetation regeneration were removed by interpolating annual July/August airborne LiDAR point clouds following ground (from 2018) and non-ground (all other years) return classification to 0.25 m cells between a height range of 5 m and 40 m from ground classified returns in 2018. “Pits” (or empty cells in burned tree canopies) were infilled to a maximum of 1 additional pixel, and trees were re-classified to ‘null’ or NoData.

In addition to 2D image analysis, structure from motion (SfM) 3D point clouds were also derived from overlapping images in Pix4Dmapper (Pix4D, Switzerland) and then processed in TerraScan (TerraSolid, Finland). To ensure comparability between SfM point clouds, data were manually shifted and aligned with airborne LiDAR data collected in 2018 using QT Modeller (Applied Imagery, United States). RPAS SfM-derived vegetation height was measured within plots (coincident to field data collection) from ground to the mean of the maximum vegetation height in each plot. Plots located at the edges of the RPAS point clouds were removed to limit edge effects and minimize the influence of distortion.

6. Statistical methods and models

To compare changes between plots and between sites, Shapiro-Wilk and Kolmogorov-Smirnov tests were used to establish data normality. Significant differences ($p \leq 0.05$) between plots/sites were determined using a two-sample *t*-test with unknown variance (parametric data). or the Wilcoxon sign-rank test when data were non-parametric. Relationships were determined (e.g. between plot and RPAS data) using linear regression. Finally, two-way ANOVA (with an F test) was used to determine the influence of study site location and time since fire on mean vegetation height, PLOTgcc, and lodgepole pine seedling density at the peak of the growing season of each year. In 2020, two-way ANOVA was used to determine if field-measured VWC (classified as low, low-medium, medium-high, and high) and study site location significantly influenced vegetation height and PLOTgcc.

7. Results

7.1. Inter-annual climate variability prior to and following the kenow fire

Mean annual air temperature and precipitation at Waterton Park gate varied considerably during the period of measurements (Fig. 3). A prolonged wetter and warmer period was observed from 2003 to 2013, approximately coinciding with increasing strength of the negative phase of the Pacific Decadal Oscillation (PDO) (also observed ~ 200 km to the northwest in the regionally proximal Columbia Valley of the Kootenay Mountains, British Columbia; Rodrigues et al., 2024; NOAA, 2024). A period of warmer, drier years began in 2014, increasing the moisture deficit within the park leading up to the Kenow fire in 2017. The year of the Kenow fire was not extremely warm or dry (only slightly warmer and drier than average). However, the cumulative moisture deficit from previous years, combined with high biomass and moss accumulation within the park contributed to a high combustible fuel load at the time of fire (Fig. 1b). This resulted in the subsequent decimation of mature conifer species and loss of organic soils, often down to mineral or bedrock layers (Gerrand et al., 2021).

With the exception of 2019, the years following the fire were both warmer and drier than the long-term average (Fig. 3). Growing season precipitation was 183 mm lower than average in 2020, while air temperatures were up to 1.4 °C above average in 2021.

Table 2 summarizes local meteorological and drought conditions in the years following the Kenow fire to 2022 at the dry and moist sites using moist site meteorological data. Mean annual air temperature and growing season temperature increased during the years following fire, with 2021 having the highest air temperature and lowest growing season precipitation. By 2022, total annual precipitation increased by about 50 % of the previous year, resulting in warmer and wetter conditions at the site. However, conditions remained drier than the 33-year long-term average precipitation for the Cameron Valley (1380 mm) (Agriculture and Irrigation, Alberta Climate Information Service (ACIS), 2022). Timing of the snow-free period varied each year with the earliest occurring May 30th, 2019, and later snow-free period starting 4–7 days later from 2020 to 2022.

7.1.1. Post-fire vegetation species composition

In the first-year post-fire (2018), regenerating vegetation was comprised of short herbaceous species with high proportions of bare ground (51 %) and coarse woody debris (10 %). Herbaceous vegetation remained dominant in 2020, however, woody vegetation had established in small proportions (2 %) at the moist site (Fig. 4). In contrast, the dry site contained a larger proportion of lodgepole pine seedlings and fireweed, with the majority of the site remaining bare. Herbaceous vegetation in the dry site was composed of forbs with no graminoid species identified, while the moist site was composed of a mix of forbs (63 %) and graminoids (31 %). Species richness in the moist site decreased from 2018 where 34 species were present (21 identified and

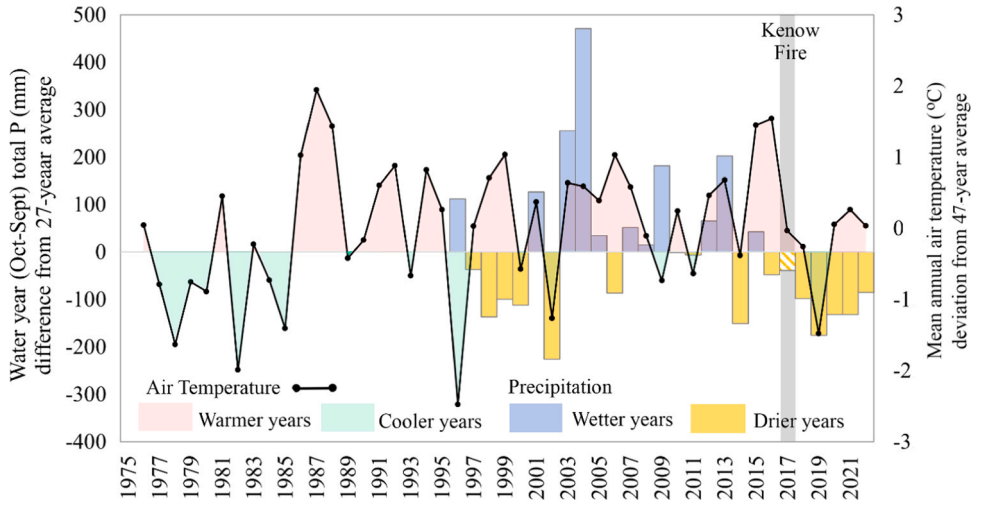

Fig. 3. Water year cumulative precipitation deviation from the 27-year average and mean annual air temperature deviation from the 47-year average (due to data availability) at the Waterton Park Gate, Alberta. A period of warm, wet conditions is illustrated from 2003 to 2013, with warmer, drier conditions after 2014, including the year of the Kenow Fire in 2017.

Table 2
Meteorological data collected within the moist site (precipitation, P) and at the Akamina #2 climate station near Cameron Lake (air temperature, snow depth, snow water equivalent (SWE)). Here, growing season is defined from May 1st to September 30th of each year, which approximates the snow-free period. Palmer drought index is also included, where + 1–4 = increasingly wet to extremely wet and −1 to −4 = increasingly dry to extremely dry (Agriculture and Irrigation, 2021).

Year	Cumulative P (mm)	Mean annual air temperature (°C)	Growing season total P (mm)	Growing season mean temperature (°C)	Maximum SWE (mm)	Maximum snow depth (cm)	Ave water year Palmer Drought Index
2019	858	1.4	434	10.6	296	137	0
2020	910	1.9	328	11.1	715	199	−2
2021	866	2.9	307	11.9	463	143	−3
2022	1298	2.1	415	11.3	372	131	−1

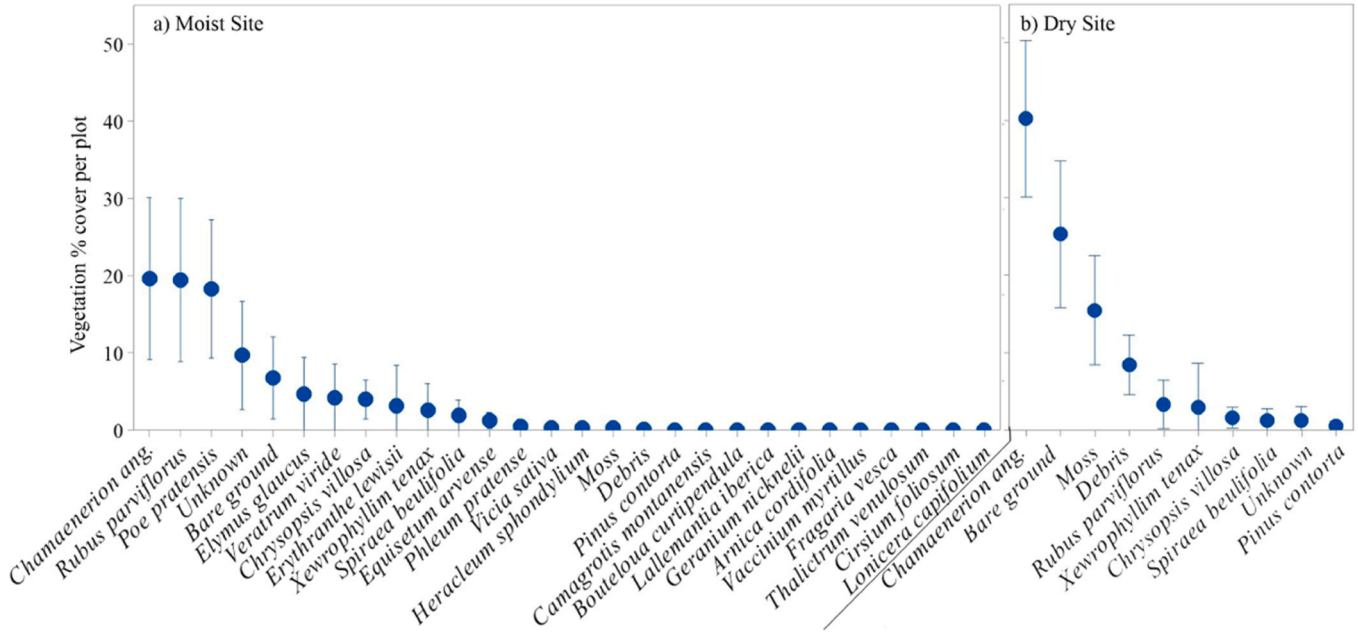

Fig. 4. Average and SD (all plots per site) of species canopy cover and other ground covers (including species that could not be identified due to immature status (unknown), bare ground, debris, and moss species) in 2020 at a) moist and b) dry sites for species where the average across each site is greater than 1 %.

13 unidentified) to 24 species (17 species identified and seven unidentified) in 2020. In the dry site, nine species were identified in 2020, revealing much lower species richness compared to the moist site.

In the summer of 2020, lodgepole pine seedling counts ranged from 0 to 2 seedlings per plot in the moist site and 0–16 seedlings per plot in the dry site (Table 3). In total, nine seedlings were counted in the moist

Table 3
Density of lodgepole pine seedlings in moist and dry sites per year.

Year	Average seedling density (SD)	
	Moist site (m^{-2})	Dry site (m^{-2})
2020	0.21 (0.44)	2.45 (3.32)
2021	0.09 (0.30)	2.97 (3.53)
2022	0.22 (0.54)	3.95 (5.64)

site, while 142 were counted in the dry site, that year. Seedling density was negatively impacted by hot, dry growing conditions in 2021, where a total of four live seedlings were counted in the moist site and 124 in the dry site respectively. Seedling counts increased to 10 and 127 indicating some recovery in 2022.

7.1.2. Variations in post-fire vegetation recovery and seasonal trends

Year to year variations in vegetation phenology including: the onset of growth, timing of peak height and cover, and the period of productivity occurred between the moist and dry sites (Fig. 5; Table 2). Average microplot vegetation height (Fig. 5a) and canopy cover (PLOTgcc) (Fig. 5b) were consistently greater (with the exception of PLOTgcc in 2022) in the moist site compared with the dry site. In 2019, the average height of vegetation in the moist site was 0.39 m (SD = 0.16 m), and, by 2020, this increased to 0.68 m (SD = 0.18 m). Moist site PLOTgcc index increased significantly from 2019 to 2020 by 0.05 (Wilcoxon, $p < 0.001$), while cover expansion (PLOTgcc) slowed as short herbaceous ground cover vegetation filled in openings between plants during the same period (Wilcoxon, $p = 0.04$). PLOTgcc peaked for most years during the 2nd week in July (~JD 195–200), while vegetation height at both sites peaked near the end of July (~JD 210).

The 2021 growing season was abnormally warm and dry, resulting in growth of vegetation earlier in the season, reaching maximum height and cover (determined from PLOTgcc) on about JD 189. Maximum height in 2021 occurred ~21 days earlier, while maximum PLOTgcc occurred 7–10 days earlier than other years. Despite earlier leaf flush/growth, height and cover remained lower in 2021, four years post-fire than in 2019 (Fig. 5a, b). Visible browning of foliage due to pine seedling mortality occurred due to heat stress, resulting in an overall reduction in both height and PLOTgcc at both sites. Vegetation growth recovered slightly in 2022 with increased growing season total precipitation and lower air temperature (Table 2).

During the period of study, biomass was greatest in the moist site in 2019 (average = 335 g m^{-2}), declining by (average) 37 g m^{-2} in 2021, with some recovery in 2022 (Fig. 6). In the dry site, biomass was significantly greater in 2020 than in 2021 ($F(1,8) = 18.72$, $p = 0.003$), with greater variability in 2022, though average biomass was slightly lower. Despite the increased biomass accumulation in the moist site compared to the dry site, there were no significant differences in biomass between the two sites ($F(1,18) = 3.08$, $p = 0.10$).

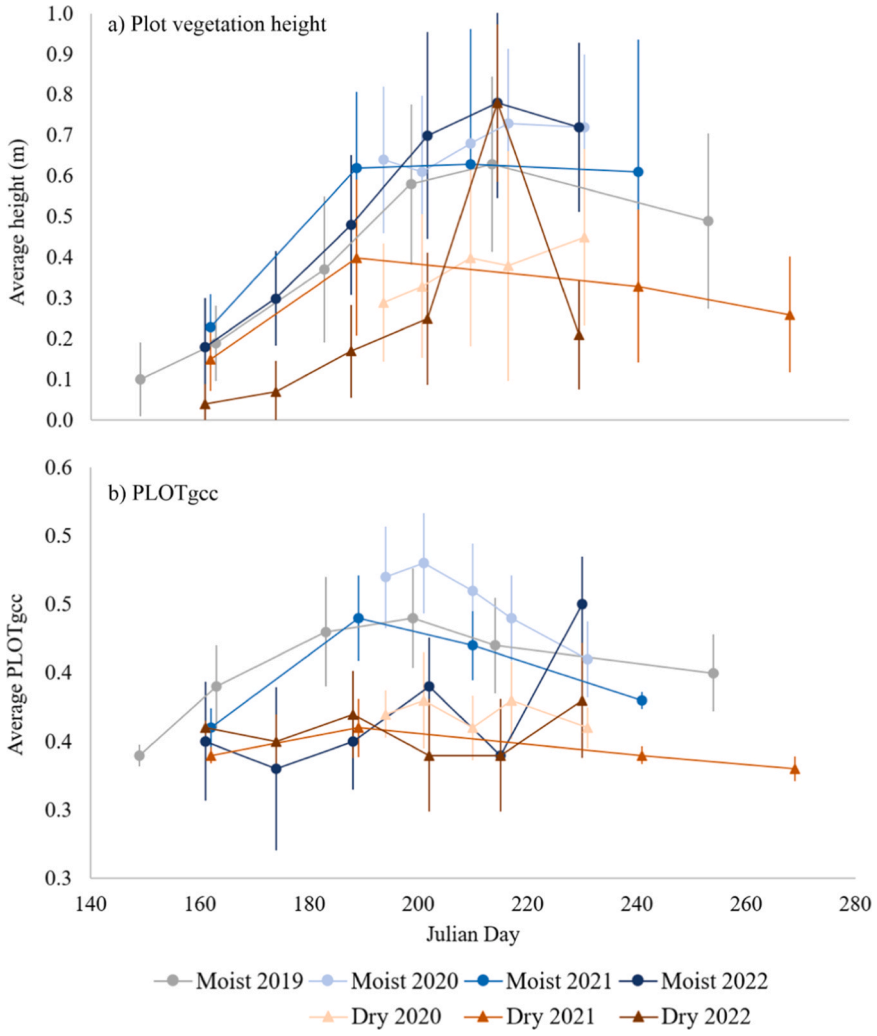

Fig. 5. Variations in average a) vegetation height and b) PLOTgcc (and SD (error bars)) within plots from 2019 to 2022 in the moist site and from 2020 to 2022 in the dry site collected approximately every 2–3 weeks during the growing season.

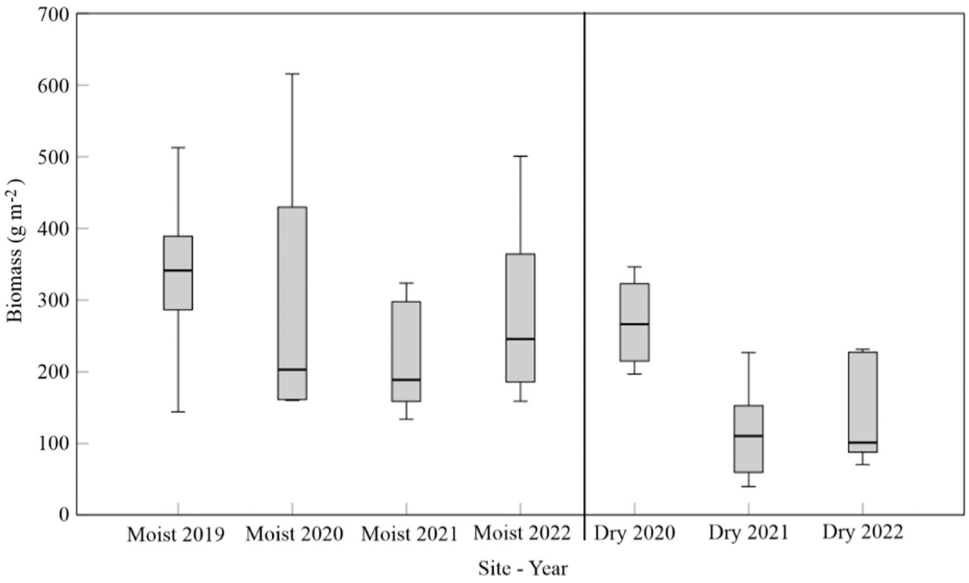

Fig. 6. Harvested, dried biomass in moist and dry sites. Boxes represent the 1st quartile, mean line, and 3rd quartile, while whiskers represent 5th and 95th percentiles. The reduction of biomass in 2021, especially in the dry site relative to 2020 is observed within the harvested plot biomass range and means.

7.1.3. Environmental Drivers of Early Post-Fire Recovery

Site location (the environmental conditions of each site) and year (weather) significantly interacted to impact mean canopy cover (PLOTgcc) ($F(1, 120) = 10.32$, $p = 0.002$) but did not have a significant impact on vegetation height. When considered individually, site location was more significant ($p < 0.001$) than year ($p = 0.47$) on mean vegetation height. Similarly, site location was also more significant ($p < 0.001$) than year ($p = 0.70$) on lodgepole pine seedling density, where average density varied between 1733 stems per ha (moist site) and 31,233 stems per ha (dry site) (Table 3).

The average soil bulk density for all plots increased from 0.58 g cm^{-3} (SD = 0.20, n = 52) at 0–5 cm depth to 0.95 g cm^{-3} (SD = 0.21, n = 37) at 10–15 cm depth (reduction in n due to encountering bedrock). Average bulk density at the 5–10 cm depth was significantly different between the moist (0.75 g cm^{-3}) and dry site (0.91 g cm^{-3}) ($p = 0.048$). Vegetation height within the dry site was positively correlated with bulk density at 10–15 cm depth ($R^2 = 0.40$, $p = 0.02$, n = 13), though bulk density had no significant influence on vegetation height or PLOTgcc at the moist site.

Seedlings were negatively correlated with VWC across plots in both

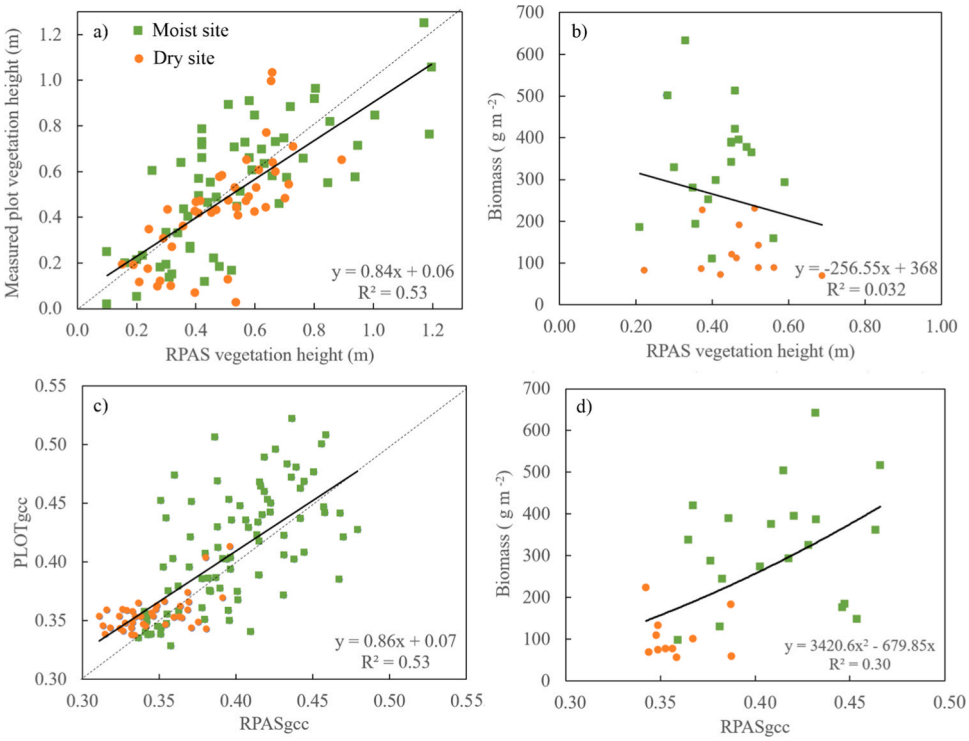

Fig. 7. Linear regressions: a) RPAS-SfM vegetation height and field height measurements; b) RPAS-SfM vegetation height and harvested biomass; and c) RPASgcc and PLOTgcc. 2nd order polynomial regression d) RPASgcc and harvested biomass through 0, used to model biomass from RPASgcc. Dashed line in a) and c) represent 1:1 line.

sites (Kendall's tau-b = −0.37, p = 0.001) and PLOTgcc (Kendall's tau-b = −0.35, p = 0.001), indicating reduced density in areas of higher soil moisture and foliage cover from regenerating species. Seedling density increased in areas with higher soil bulk density at 5–10 cm depth (Kendall's tau-b = 0.24, p = 0.031, n = 49) found in the dry site where highest density of seedlings were found.

7.1.4. Use of RPAS photogrammetry and SfM for quantifying early post-fire vegetation change

RPAS SfM-based height illustrated in Fig. 7a corresponded well with average microplot height measurements ($p < 0.001$) but did not correspond with harvested biomass (Fig. 7b). SfM heights corresponded better with field heights in the dry site ($R^2 = 0.54$; SD = 0.17 m) relative to the moist site ($R^2 = 0.49$; SD = 0.18 m), with greater differences observed in plots containing the shortest vegetation (up to 0.20 m) and taller vegetation exceeding 0.80 m.

RPASgcc [Eq. 1] corresponded well with PLOTgcc from RGB photography ($p < 0.001$) (Fig. 7c). Greater PLOTgcc occurred in moist plots (ranging from ~0.33–0.47) compared with the dry plots (0.31 – 0.40) with increased deviation from measured with increasing canopy cover. RPASgcc had greater range of variability of vegetation cover than PLOTgcc within the dry site, varying between 0.33 and 0.37 (PLOTgcc) and between 0.31 and 0.39 (RPASgcc) within the moist site. RPASgcc is significantly correlated with harvested biomass ($p < 0.001$) based on the 2nd order polynomial.

Biomass was modelled across the time series of surveyed areas based on the RPASgcc using the regression equation in Fig. 7d (SE = 14.7 g m^{-2}) illustrated in Fig. 8. Post-fire biomass accumulation occurred mostly in topographically low-lying areas in the years following fire, especially in the dry site. In the moist site, topographical depressions contained standing water into late June and become dry by mid-July, providing an opportunity for rapid herbaceous and sedge growth (Fig. 8f-i) and along the trail northwest of both sites. Mineral soil outcrops with low organic matter (southern part of the moist site (Fig. 8h)) had reduced biomass accumulation during the abnormally dry/warm summer of 2021. Average biomass across the RPAS survey area is 233 g m^{-2} (average SD = 126 g m^{-2}, moist site) and 84 g m^{-2} (average SD = 101 g m^{-2}, dry site). Similar to field measurements, biomass decreased in 2021 from July to August by 43 and 61 g m^{-2}(average), at moist and dry sites, respectively due to drying and mortality by mid-August. In comparison, 2022 was wetter (Table 2) and vegetation biomass increased by 91 and 48 g C m^{-2} at moist and dry sites (on average) in August 2022.

8. Discussion

This study assessed the impact of a prolonged period of warm, dry weather (interannual climate) on post-fire vegetation regeneration and seedling recruitment within moist and dry endmember sites in a montane valley in southern Alberta. The research has implications for forest management in Canada as montane forests including seedlings and the herbaceous understory following fire may be impacted by prolonged dry conditions. Here moderate fires, such as those that existed in Waterton more than 100 years ago, especially along high fire severity margins (Barrett, 1996) may be a potential mechanism for reducing the impacts of 19th and 20th century colonial/settler forest management practices, promoting species heterogeneity and ecosystem resilience to fire (e.g. Mori and Lertzman, 2011; Coogan et al., 2021; Stockdale et al., 2019; Eisenberg et al., 2019). In another mountain site approximately 100 kms north of Waterton, Stockdale et al. (2019) show that restoration of grassland patches observed in the early 1900's reduced the probability of high intensity fire by almost half. However, this also depends on the timing and location of the ignition and vegetation type distribution.

Are lodgepole pine forests and understory herbaceous vegetation burned by high intensity fire resilient to drought in the years following the Kenow wildfire? We show that seedling growth proliferated on dry mineral soils similar to findings from other studies (e.g. described in Lotan et al., 1985) and during prolonged, multi-year drought. Herbaceous vegetation was extensive in the moist study site and was less resilient to drought, resulting in reduced biomass production, with

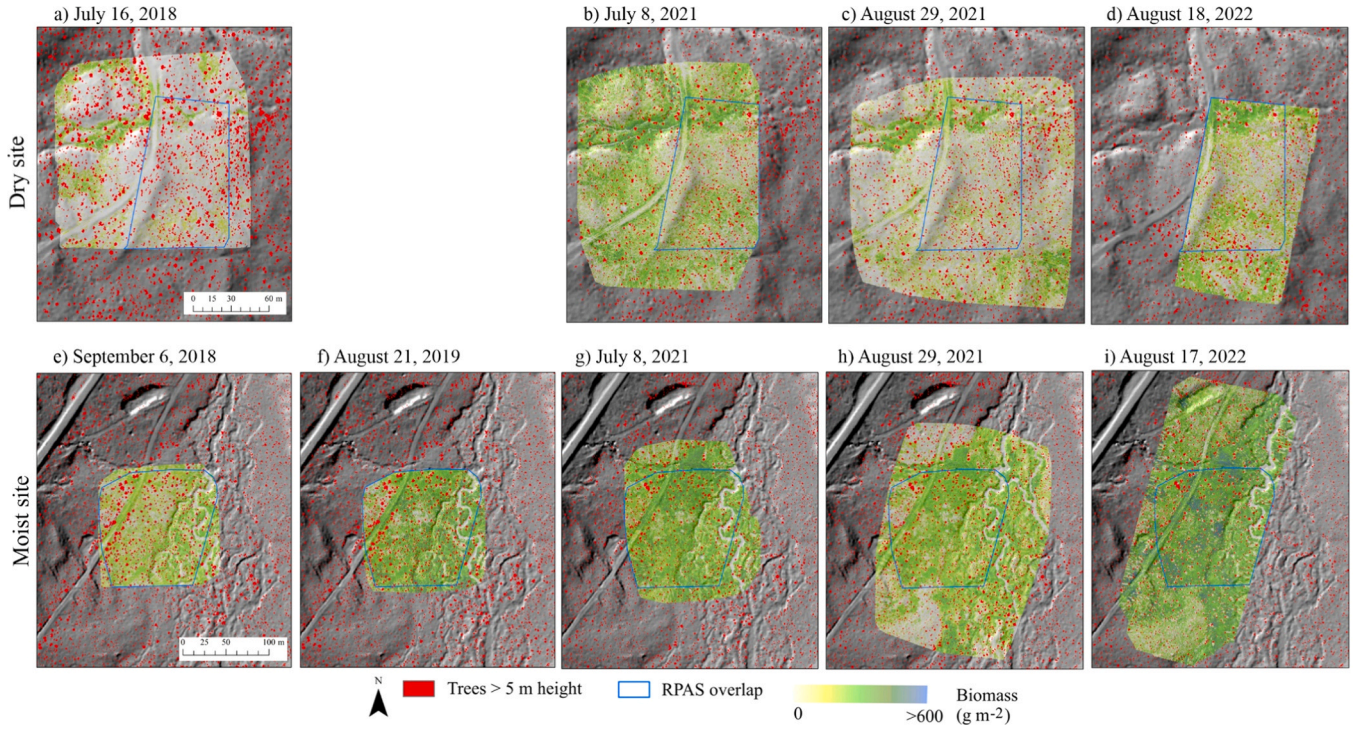

Fig. 8. Time-series biomass modelled from RPASgcc within dry and moist sites for each date of data collection. Modelled biomass is overlaid onto a hillshade model (to illustrate topographic position, roughness) and excludes standing burned tree stems and branches (red), which could alter RPASgcc. Outlined areas (blue) indicate areas with overlapping RPAS imagery.

recovery in following years. This also corresponds with early post-fire research by Eisenberg et al. (2019) who show that prairie and aspen ecosystems one year following the Kenow fire at Waterton were resilient to extreme fire behaviour. Despite our results, we recognize that pine recovery is highly heterogeneous (Guz et al., 2021) and more research is required to better understand growth dynamics throughout the valley and with burn severity, which will provide a greater overall understanding of forest resilience. The following discussion describes our results within the context of the broader literature within the context of highly variable climatic gradients found in the south-eastern Canadian Rocky Mountains.

8.1. Drought impacts on post-fire establishment of herbaceous vegetation and seedling recruitment

Inter-annual climate variability can alter herbaceous vegetation growth and the condition of conifer seedlings (Andrus et al., 2018; Busby et al., 2020; Dodson et al., 2013; Rother, 2015), while other studies have shown that lodgepole pine can be impacted by drought conditions via regeneration lag (Harvey et al., 2016). Moisture in the years following the Kenow fire was below the long-term mean due to low total precipitation and higher than average air temperatures (Fig. 3). These conditions resulted in moderate to severe drought conditions from 2020 to 2022 (Table 2). Within the longer-term climatological record, Waterton experienced above average air temperatures in nine of the last 10 years and below average precipitation in seven of the last 10 years. Over the longer term, summer 2021 was the driest period of the study (Fig. 5), second driest in 26 years, and the second warmest in 47 years.

The impacts of abnormally warm, dry conditions are locally affected by microtopography and soil bulk density, which impact growth of early successional species (Fig. 8). Post-fire regeneration of herbaceous vegetation can reduce climatological and hydrological limitations on vegetation recovery by moderating site conditions, masking the albedo effects from charred soils, increasing the proportion of latent energy exchanges, and reducing runoff/nutrient losses (Harvey et al., 2016). For example, Davis et al. (2019) observed that extremes in temperature and vapour pressure deficit were reduced in forests with overstory canopy of more than 50 % cover, with biological implications to understory vegetation. The reduction of climatic extremes in Davis et al. (2019) were also strongly dependent on plot water balance, which is predicted to reduce over time due to the potential for greater drying and water deficits with increased warming (Dawe et al., 2022). Near surface soil and air temperature ranges during diurnal periods were also reduced in areas containing moist soils, providing more optimal conditions for micro-refugia than sites experiencing dry conditions and larger temperature ranges and effects from canopy cover and topography (Ashcroft and Gollan, 2013). This could have implications to micro-climate variability, species composition, and C uptake. In this study, the moist site accumulated more herbaceous vegetation compared to the dry site, resulting in greater species diversity, height, canopy cover, and biomass (Figs. 4–6, 8), which likely reduced sensible heating from charred soil surfaces.

Greater lodgepole pine recruitment in the dry site corresponded with high density of pre-fire mature lodgepole pine (60 % of tree species found within the sites) and establishment of lodgepole pine on dry mineral soils. Harvey et al. (2016) found that distance to seed source has the greatest impact on post-fire lodgepole pine establishment. While we did not examine the numbers of open cones/cone availability, crown fire and high density of lodgepole pine (Gerrand et al., 2021) likely contributed to early recruitment (Talucci et al., 2019). High wind speeds (sometimes gusting >100 km hr^{-1}) also occur within the valley, with prevailing wind directions originating from south to north through the valley. A stand of unburned lodgepole pine and mixed conifer tree species approximately 200–300 m south of the sites may also have contributed airborne seeds to the sites via wind gusts. There were no other surviving trees within the Cameron Valley proximal (within a few kilometers) of the field sites.

In the early years post-fire at Waterton, Engelmann spruce and subalpine fir were not observed within microplots. Moist soil and the accumulation of coarse woody debris provide favourable microsite conditions for Engelmann spruce (Hill and Ex, 2020), however, warmer, drier conditions may reduce Engelmann spruce recruitment and survival resulting in elevation range contraction (Conlisk et al., 2017) yet to be observed. Shade from regenerating herbaceous species can reduce the impacts of the cumulative effects from soil warming and drought conditions following fire. Further subalpine fir prefer shade conditions (e.g. Conlisk et al., 2017; Goke and Martin, 2023), while Engelmann spruce prefer canopy gaps. Gerrand et al. (2021) found greater density of mature (burned) Engelmann spruce within the moist site. Lodgepole pine seedling density ranged from ~1700 to 31,000 seedlings ha^{-1} (average) and were mostly found in charred mineral soils within the dry site (Fig. 4). Lodgepole pine densities at Yellowstone National Park (USA), for example, ranged from ~29,000–60,000 stems ha^{-1} (Turner et al., 1997, 2004) and ~33,000 stems ha^{-1} on average, six years post-fire in Glacier National Park (Harvey et al., 2016). Timing of peak establishment for conifers ranged from between six years (Glacier National Park) and 12 years (Yellowstone National Park) following fire (Harvey et al., 2016), with early successional species: lodgepole pine and subalpine fir typically establishing within 2–4 years of fire.

8.2. Implications of vegetation trajectories on post-fire biomass accumulation and carbon

Carbon (C) emissions from wildland fire (and other disturbances) are significant (e.g. Meigs et al., 2009; Wang et al., 2021), shifting Canadian forests from a sink for atmospheric C to a source during years with large areas burned (Kurz et al., 2008). Crown fire results in foliage and partial branch and bark combustion (e.g. Talucci and Krawchuk 2019). Remaining burned biomass contributes to long-term C emissions or soil C pools (e.g. Gerrand et al., 2021).

Combined above and below ground carbon losses during the Kenow Wildland Fire were between 11 kg C m^{-2} and ~7 kg C m^{-2} for the moist and dry sites, respectively, observed in Gerrand et al., (2021). Approximately 16 % (moist) and 17 % (dry) of total C losses were from tree biomass combustion during fire, with the remainder from soil organic matter and mosses. Regenerating vegetation in 2019, 2021, and 2022 (Fig. 6) sequestered between ~0.6 %, (0.048 kg C m^{-2}) to 1.5 % (0.169 kg C m^{-2}) of C losses from combustion at the dry and moist sites, respectively (Gerrand et al., 2021). Dry conditions and the mortality of vegetation in 2021 reduced C sequestration by 42 %, relative to 2019–2020 (Figs. 6, 8). Despite limited C storage, annual rate of growth of herbaceous vegetation (gross primary productivity) has been rapid. The accumulation of 250 g m^{-2} of biomass in the moist site by year five (Fig. 6) is greater than biomass accumulated after 11 years at Yellowstone National Park (340 g m^{-2}) and exceeds sagebrush accumulation (208 g m^{-2}) after five years in Southern Idaho (Fellows et al., 2018; Turner et al., 2016).

8.3. Supplementing field measurements with RPAS to monitor ecosystem recovery

The utility of RPAS SfM and photogrammetric methods for monitoring vegetation change and recovery has made it a popular, inexpensive method for data collection, especially in poorly accessible mountain environments. Numerous studies have illustrated the use of SfM point clouds for measuring vegetation height, cover, and species (Goodbody et al., 2017, 2018; Nuijten et al., 2019). Classification of lodgepole pine from herbaceous vegetation was not possible during this study (to year 5, post fire) due to occlusion of seedlings by the herbaceous understory canopy, while other attributes including height and cover of vegetation were more easily estimated. Quantifying vegetation height requires accurate ground elevation data, which is not possible using

photogrammetric methods in closed understory/herbaceous canopies, due to an inability to observe the ground from multiple directions. This introduces uncertainty in estimating vegetation height resulting in underestimation of height for short vegetation (e.g. Fig. 7a for vegetation < 0.4 m tall) (James et al., 2017). To minimize terrain elevation and vegetation height uncertainties due to ground occlusion, it is important to complete ground surveys before significant vegetation regeneration, typically within the first year following fire.

While short, dense herbaceous cover made it more difficult to estimate biomass from SfM point clouds in the early years post-fire, the use of the green chromatic coordinate (GCC) shows promise, especially where scorched ground is still visible within photographs (Fig. 7). RPASgcc correlated with PLOTgcc determined from photographs ($R^2 = 0.53$) and with harvested biomass ($R^2 = 0.30$). Originally developed for oblique photography and videography of vegetation phenology on towers (Richardson et al., 2009), visible photographic indices such as GCC have been used as a simple, effective method for quantifying vegetation cycles and change. For example, Peichl et al. (2015) used RGB photographs to calculate GCC, which compared well with gross ecosystem productivity and net ecosystem exchange observed using eddy covariance methods. Similar observations were made by Larrinaga and Brotons (2019) who used RPAS GCC to monitor regenerating pine species following fire in Spain. GCC correlated with diameter at breast height, which is a volumetric proxy often used to estimate biomass. Here, RPASgcc was used to estimate spatial and temporal variations in biomass within moist and dry sites (Fig. 8). While there is considerable variability between RPASgcc and harvested biomass at the plot scale, the overall spatial distribution of post-fire biomass accumulation within the sites can be used to quantify post-fire vegetation trajectories. Future studies should acquire RPAS photogrammetric data across a broader range of site conditions, enabling improved understanding of localized environmental drivers of vegetation stress, resilience, and growth to expand and up-scale sampling beyond plots.

9. Conclusions

This study investigated the first five years of post-fire vegetation regeneration in moist and dry endmember mountain valley sites, during an abnormally warm and dry period. In the early years following the Kenow fire, herbaceous vegetation regeneration was greater in the moist site compared to the dry site. However, lodgepole pine seedling establishment and growth were more prolific in the dry site. As expected, both sites experienced declines in herbaceous vegetation biomass in 2021 due to severe hot and dry conditions. Although not to the same degree, conifer seedlings also demonstrated sensitivity to the abnormally warm and dry conditions. This resulted in mortality of seedlings in the dry site and seedling recovery the following year. Other conifer species (subalpine fir and Engelmann spruce) had not been observed in either site, though this may be due to the timing of this early post-fire period. Future research should consider the recovery of other species and over broader areas that are representative of the valley to determine how patch dynamics could vary over longer time periods.

Monitoring post-fire recovery is time consuming and can be impractical or hazardous within difficult to access locations. RPAS surveys can enhance ecosystem regeneration monitoring over larger areas compared with using field plots. The efficacy of RPAS should also improve as seedlings become more separable based on height, cover, and spectra from the surrounding ground and herbaceous vegetation over time since fire. Here, repeated deployment of RPAS over a range of regeneration plot characteristics provided data on the spatial impact of drivers of ecosystem recovery rates and resilience. Furthermore, photogrammetric RGB indices and SfM of cover and vegetation height enable modelling of vegetation trajectories and the accumulation of biomass, which can be linked to ecosystem function, including mass and energy exchanges over time.

CRediT authorship contribution statement

J. Aspinall: Writing – review & editing, Writing – original draft, Visualization, Validation, Methodology, Investigation, Formal analysis, Conceptualization. **L. Chasmer:** Writing – review & editing, Writing – original draft, Visualization, Validation, Supervision, Resources, Project administration, Methodology, Investigation, Funding acquisition, Formal analysis, Data curation, Conceptualization. **C.A. Coburn:** Writing – review & editing, Methodology, Investigation, Conceptualization. **C. Hopkinson:** Writing – review & editing, Supervision, Software, Resources, Project administration, Methodology, Investigation, Funding acquisition, Data curation, Conceptualization.

Declaration of Competing Interest

The authors declare that they have no known competing financial interests or personal relationships that could have appeared to influence the work reported in this paper.

Acknowledgements

Research was conducted on the traditional territorial lands of the Siksikaitsitapi (Blackfoot) people, who have a long history prior to the formation of Waterton Lakes National Park. The authors would like to acknowledge funding from Parks Canada, Waterton Lakes National Park (grant number GC-1158), Canada Wildfire NSERC-SPG-N, RE5005090, Alberta Innovates, NSERC Discovery Grant funding to Chasmer (grant number 2017–04492) and Hopkinson (grant number 2017–04362) and a University of Lethbridge Start-up Grant to Chasmer. The Teledyne Optech Inc. Titan lidar system was purchased via a grant to Hopkinson by Western Economic Diversification Canada (grant number 000015316), GNSS and other equipment was funded by Canadian Foundation for Innovation (grant number 32436). We would like to thank Dr. Lawrence Flanagan for providing funded student field assistants, meteorological data, and advice throughout the project. Dr. Adam Collingwood is also acknowledged for enabling funding and our activities within Waterton National Park. Field support was provided by: Jacob Martin, Sam Gerrand, Apryl Nish, Kaydunn Henry, Danielle Nadeau, Henry Bain, Jessica vanGaalen, Celeste Barns, Emily Jones, Edberto Moura-Lima, Humaira Enayetullah, Nick Cuthbertson, and Rachelle Shearing. We would also like to thank two reviewers for helpful comments on writing and content suggestions.

Data availability

Data will be uploaded to the Federated Research Data Repository and a DOI will be provided

References

Agriculture and Irrigation, 2021, May 1. Alberta Climate Information Service (ACIS. Current and Historical Alberta Weather Station Data Viewer. Alberta Climate Information Service. ⟨https://acis.alberta.ca⟩.

Andrus, R.A., Harvey, B.J., Rodman, K.C., Hart, S.J., Veblen, T.T., 2018. Moisture availability limits subalpine tree establishment. Ecology 99 (3), 567–575. https://doi.org/10.1002/ecy.2134.

Ashcroft, M.B., Gollan, J.R., 2013. Moisture, thermal inertia, and the spatial distributions of near-surface soil and air temperatures: understanding factors that promote microrefugia. Agric. For. Meteorol. 176, 77–89. https://doi.org/10.1016/j.agrformet.2013.03.008.

Assal, T.J., Steen, V.A., Caltrider, T., Cundy, T., Stewart, C., Manning, N., Anderson, P.J., 2021. Monitoring long-term riparian vegetation trends to inform local habitat management in a mountainous environment. Ecol. Indic. 127, 107807.

Axelson, J.N., Hawkes, B.C., van Akker, L., Alfaro, R.I., 2018. Stand dynamics and the mountain pine beetle—30 years of forest change in Waterton Lakes National Park, Alberta, Canada. Can. J. For. Res. 48 (10), 1159–1170.

Barnes, C., Hopkinson, C., 2022. Quality control impacts on total precipitation gauge records for montane valley and ridge sites in SW Alberta, Canada. Data 7 (6), 73. https://doi.org/10.3390/data7060073.

Barnes, C., MacDonald, R.J., Hopkinson, C., 2025. Montane Seasonal and Elevational Precipitation Gradients in the Southern Rockies of Alberta, Canada. Hydrol. Process. 39 (1), e70061.
Barrett, S.W., 1996. The historic role of fire in Waterton Lakes National Park, Alberta. Parks Canada, Ottawa, Ont., Rep. KWL-30004.
Busby, S.U., Moffett, K.B., Holz, A., 2020. High-severity and short-interval wildfires limit forest recovery in the central cascade range. Ecosphere 11 (9), e03247. https://doi.org/10.1002/ecs2.3247.
Caratti, J.F., 2006. Gen. Tech. Rep. Point intercept sampling method. USDA Forest Service. RMRS-GTR-164-CD. ⟨www.fs.fed.us/rm/pubs/rmrs_gtr164⟩.
Carter, M.R., Gregorich, E.G. (Eds.), 2008. Soil sampling and methods of analysis. CRC Press, Boca Raton, Fla. https://doi.org/10.1201/9781420005271.
Chen, H.Y., Légaré, S., Bergeron, Y., 2004. Variation of the understory composition and diversity along a gradient of productivity in Populus tremuloides stands of northern British Columbia, Canada. Can. J. Bot. 82 (9), 1314–1323.
Conlisk, E., Castanha, C., Germino, M.J., Veblen, T.T., Smith, J.M., Kueppers, L.M., 2017. Declines in low-elevation subalpine tree populations outpace growth in high-elevation populations with warming. J. Ecol. 105 (5), 1347–1357. https://doi.org/10.1111/1365-2745.12750.
Coogan, S.C., Daniels, L.D., Boychuk, D., Burton, P.J., Flannigan, M.D., Gauthier, S., Kafka, V., Park, J.S., Wotton, B.M., 2021. Fifty years of wildland fire science in Canada. Can. J. For. Res. 51 (2), 283–302. https://doi.org/10.1139/cjfr-2020-0314.
Coop, J.D., Massatti, R.T., Schoettle, A.W., 2010. Subalpine vegetation pattern three decades after stand-replacing fire: effects of landscape context and topography on plant community composition, tree regeneration, and diversity. J. Veg. Sci. 21 (3), 472–487. https://doi.org/10.1111/j.1654-1103.2009.01154.x.
Daniels, L.D., Maertens, T.B., Stan, A.B., McCloskey, S.P.J., Cochrane, J.D., Gray, R.W., 2011. Direct and indirect impacts of climate change on forests: three case studies from British Columbia. Can. J. Plant Pathol. 33 (2), 108–116. DOI: 10.1080/07060661.2011.563906.
Davis, K.T., Dobrowski, S.Z., Holden, Z.A., Higuera, P.E., Abatzoglou, J.T., 2019. Microclimatic buffering in forests of the future: the role of local water balance. Ecography 42, 1–11. https://doi.org/10.1111/ecog.03836.
Dawe, D.A., Parisien, M.-A., Dongen, A. van, Whitman, E., 2022. Initial succession after wildfire in dry boreal forests of northwestern North America. Plant Ecol. 0123456789. https://doi.org/10.1007/s11258-022-01237-6.
Eisenberg, C., Anderson, C.L., Collingwood, A., Sissons, R., Dunn, C.J., Meigs, G.W., Hibbs, D.E., Murphy, S., Kuiper, S.D., SpearChief-Morris, J., Little Bear, L., 2019. Out of the ashes: ecological resilience to extreme wildfire, prescribed burns, and indigenous burning in ecosystems. Front. Ecol. Evol. 7, 436.
Environment Canada, 2022. *Historical Data.* Government of Canada. Hourly Data Report for July 19, 2023. Climate - Environment and Climate Change Canada (weather.gc.ca).
Feddema, J.J., Mast, J.N., Savage, M., 2013. Modeling high-severity fire, drought and climate change impacts on ponderosa pine regeneration. Ecol. Model. 253, 56–69. https://doi.org/10.1016/j.ecolmodel.2012.12.029.
Fellows, A.W., Flerchinger, G.N., Lohse, K.A., Seyfried, M.S., 2018. Rapid recovery of gross production and respiration in a mesic mountain big sagebrush ecosystem following prescribed fire. Ecosystems 21 (7), 1283–1294. https://doi.org/10.1007/s10021-017-0218-9.
Fisher, G.M., 1935. Comparative germination of tree species on various kinds of surface soil material in the western white pine type. Ecology 16, 606–611.
Gerrand, S., Aspinall, J., Jensen, T., Hopkinson, C., Collingwood, A., Chasmer, L., 2021. Partitioning carbon losses from fire combustion in a montane valley, Alberta Canada. For. Ecol. Manag. 496, 119435. https://doi.org/10.1016/j.foreco.2021.119435.
Goke, A., Martin, P.H., 2023. Drought-induced photosynthetic decline and recruitment losses are mediated by light microenvironment in Rocky Mountain subalpine forest tree seedlings. For. Ecol. Manag. 546, 121295. https://doi.org/10.1016/j.foreco.2023.121295.
Goodbody, T., Coops, N.C., Hermosilla, T., Tompalski, P., Crawford, P., 2018. Assessing the status of forest regeneration using digital aerial photogrammetry and unmanned aerial systems. Int. J. Remote Sens. 39 (15-16), 5246–5264. https://doi.org/10.1080/01431161.2017.1402387.
Goodbody, T., Coops, N.C., Marshall, P.L., Tompalski, P., Crawford, P., 2017. Unmanned aerial systems for precision forest inventory purposes: a review and case study. For. Chron. 93 (1), 71–81. https://doi.org/10.5558/tfc2017-012.
Guz, J., Gill, N.S., Kulakowski, D., 2021. Long-term empirical evidence shows post-disturbance climate controls post-fire regeneration. J. Ecol. 109 (12), 4007–4024.
Harvey, B.J., Donato, D.C., Turner, M.G., 2016. High and dry: Post-fire tree seedling establishment in subalpine forests decreases with post-fire drought and large stand-replacing burn patches. Glob. Ecol. Biogeogr. 25 (6), 655–669. https://doi.org/10.1111/geb.12443.
Haughian, S.R., Burton, P.J., Taylor, S.W., Curry, C., 2012. Expected effects of climate change on forest disturbance regimes in British Columbia. J. Ecosyst. Manag. 13 (1), 1–24. https://doi.org/10.22230/jem.2012v13n1a152.
Hessburg, P.F., Miller, C.L., Parks, S.A., Povak, N.A., Taylor, A.H., Higuera, P.E., Prichard, S.J., North, M.P., Collins, B.M., Hurteau, M.D., Larson, A.J., 2019. Climate, environment, and disturbance history govern resilience of western North American forests. Front. Ecol. Evol. 7, 239. https://doi.org/10.3389/fevo.2019.00239.
Hill, E.M., Ex, S., 2020. Microsite conditions in a low-elevation Engelmann spruce forest favor ponderosa pine establishment during drought conditions. For. Ecol. Manag. 463, 118037. https://doi.org/10.1016/j.foreco.2020.118037.
Hopkinson, C., Barnes, C., 2022. Precipitation gauge and supplemental weather station data for three Oldman River headwater locations in SW Alberta. Fed. Res. Data Repos. https://doi.org/10.20383/102.0551.
James, M.R., Robson, S., Smith, M.W., 2017. 3-D uncertainty-based topographic change detection with structure-from-motion photogrammetry: precision maps for ground control and directly georeferenced surveys. Earth Surf. Process. Landf. 42 (12), 1769–1788. https://doi.org/10.1002/esp.4125.
Kurz, W.A., Stinson, G., Rampley, G.J., Dymond, C.C., Neilson, E.T., 2008. Risk of natural disturbances makes future contribution of Canada's forests to the global carbon cycle highly uncertain. Proc. Natl. Acad. Sci. 105 (5), 1551–1555. https://doi.org/10.1073/pnas.070813310.
Larrinaga, A.R., Brotons, L., 2019. Greenness indices from a low-cost UAV imagery as tools for monitoring post-fire forest recovery. Drones 3 (1), 6. https://doi.org/10.3390/drones3010006.
Littlefield, C.E., 2019. Topography and post-fire climatic conditions shape spatio-temporal patterns of conifer establishment and growth. Fire Ecol. 15 (1), 1–20.
Lotan, J., Brown, J., Neuenschwander, L., 1985. Role of fire in lodgepole pine forests. In: Baumgartner, D., et al. (Eds.), Lodgepole pine the species and its management *Symposium Proceedings.* Washington State University, Pullman, pp. 133–152.
Meigs, G.W., Donato, D.C., Campbell, J.L., Martin, J.G., Law, B.E., 2009. Forest fire impacts on carbon uptake, storage, and emission: the role of burn severity in the Eastern Cascades, Oregon. Ecosystems 12, 1246–1267. https://doi.org/10.1007/s10021-009-9285-x.
Mori, A.S., Lertzman, K.P., 2011. Historic variability in fire-generated landscape heterogeneity of subalpine forests in the Canadian Rockies. J. Veg. Sci. 22 (1), 45–58. https://doi.org/10.1111/j.1654-1103.2010.01230.x.
NOAA, 2024. *ERSST PDO Index* [Data set. National Centers fo Environmental Information. ncei.noaa.gov/pub/data/cmb/ersst/v5/index/ersst.v5.pdo.dat.
Nuijten, R.J., Coops, N.C., Goodbody, T.R., Pelletier, G., 2019. Examining the multi-seasonal consistency of individual tree segmentation on deciduous stands using digital aerial photogrammetry (DAP) and unmanned aerial systems (UAS). Remote Sensing 11 (7), 739–757.
Parks Canada, 2018. Green. Scene. Retrieved from ⟨https://www.pc.gc.ca/en/pn-np/ab/waterton/nature/environment/verdure-green⟩.
Parks Canada, 2019. Fire. Retrieved from ⟨https://www.pc.gc.ca/en/pn-np/ab/waterton/nature/environment/feu-fire⟩.
Parks Canada, 2021. Fire Mt. Retrieved from ⟨https://www.pc.gc.ca/en/pn-np/ab/waterton/nature/environment/feu-fire/montagne-mountain⟩.
Peichl, M., Sonnentag, O., Nilsson, M.B., 2015. Bringing color into the picture: using digital repeat photography to investigate phenology controls of the carbon dioxide exchange in a boreal mire. Ecosystems 18, 115–131. https://doi.org/10.1007/s10021-014-9815-z.
Richardson, A.D., Braswell, B.H., Hollinger, D.Y., Jenkins, J.P., Ollinger, S.V., 2009. Near-surface remote sensing of spatial and temporal variation in canopy phenology. Ecol. Appl. 19 (6), 1417–1428. https://doi.org/10.1890/08-2022.1.
Rodrigues, I.S., Hopkinson, C., Chasmer, L., MacDonald, R., Bayley, S., Brisco, B., 2024. Multi-decadal Floodplain Classification and Trend Analysis in the Upper Columbia River Valley, British Columbia. Hydrol. Earth Syst. Sci. Discuss. 1–34. https://doi.org/10.5194/hess-28-2203-2024.
Rother, M.T., 2015. Conifer. Regen. Wildfire Low. -Elev. For. Colo. Front Range: Implic. a Warme, drier Clim. (Dr. Diss., Univ. Colo. Boulder.
Schoennagel, T., Turner, M.G., Romme, W.H., 2003. The influence of fire interval and serotiny on postfire lodgepole pine density in Yellowstone National Park. Ecology 84 (11), 2967–2978.
Stevens-Rumann, C.S., Prichard, S.J., Whitman, E., Parisien, M.A., Meddens, A.J., 2022. Considering regeneration failure in the context of changing climate and disturbance regimes in western North America. Can. J. For. Res. 52 (10), 1281–1302. https://doi.org/10.1139/cjfr-2022-0054.
Stockdale, C.A., McLoughlin, N., Flannigan, M., Macdonald, S.E., 2019. Could restoration of a landscape to a pre-European historical vegetation condition reduce burn probability? Ecosphere 10 (2), e02584.
Tackle, D., 1959. Silv. Lodg. pine (No. 19). Intermt. For. Range Exp. Station, For. Serv., US Dep. Agric.
Talucci, A.C., Krawchuk, M.A., 2019b. Dead forests burning: the influence of beetle outbreaks on fire severity and legacy structure in sub-boreal forests. Ecosphere 10 (5), e02744. https://doi.org/10.1002/ecs2.2744.
Talucci, A.C., Lertzman, K.P., Krawchuk, M.A., 2019a. Drivers of lodgepole pine recruitment across a gradient of bark beetle outbreak and wildfire in British Columbia. For. Ecol. Manag. 451, 117500.
Turner, M.G., Romme, W.H., Gardner, R.H., Hargrove, W.W., 1997. Effects of fire size and pattern on early succession in yellowstone national park. Ecol. Monogr. 67 (4), 411–433. https://doi.org/10.1890/0012-9615(1997)067[0411:EOFSAP]2.0.CO;2.
Turner, M.G., Tinker, D.B., Romme, W.H., Kashian, D.M., Litton, C.M., 2004. Landscape patterns of sapling density, leaf area, and aboveground net primary production in postfire lodgepole pine forests, Yellowstone National Park (USA). Ecosystems 7 (7), 751. https://doi.org/10.1007/s10021-004-0011-4.
Turner, M.G., Whitby, T., Tinker, D., Romme, W., 2016. Twenty-four years after the yellowstone fires: are postfire lodgepole pine stands converging in structure and function? Ecology 97 (5), 1260–1273. https://doi.org/10.1890/15-1585.1.
Wang, J.A., Baccini, A., Farina, M., Randerson, J.T., Friedl, M.A., 2021. Disturbance suppresses the aboveground carbon sink in North American boreal forests. Nat. Clim. Change 11 (5), 435–441.
Woebbecke, D.M., Meyer, G.E., Von Bargen, K., Mortensen, D.A., 1995. Color indices for weed identification under various soil, residue, and lighting conditions. Trans. ASAE 38 (1), 259–269. https://doi.org/10.13031/2013.27838.
Zehetgruber, B., Kobler, J., Dirnböck, T., Jandl, R., Seidl, R., Schindlbacher, A., 2017. Intensive ground vegetation growth mitigates the carbon loss after forest disturbance. Plant Soil 420 (1-2), 239–252. https://doi.org/10.1007/s11104-017-3384-9.